Cyclic Large Displacement Analysis of Steel Tubular Bridge Piers under Combined Axial and Bidirectional Lateral Loading

Iraj H.P. Mamaghani
Associate Professor
Dept. of Civil Engineering
University of North Dakota
USA

Fokruddin Ahmad

Basha Dorose

Graduate Student
Dept. of Civil Engineering
University of North Dakota

Abstract

This paper deals with the large displacement analysis of thin-walled steel tubular bridge piers subjected to cyclic bidirectional lateral loading in the presence of constant axial load. In comparison with the behavior of such piers under conventional cyclic unidirectional lateral loads, the deterioration in strength and ductility caused by severe cyclic lateral bidirectional loads is examined based on nonlinear finite-element analysis and test results. Pseudo dynamic bidirectional tests, available in the literature, are used to substantiate the accuracy of the finite-element analysis. The results confirm the importance of considering the behavior of steel tubular bridge piers under bidirectional lateral loading. The bidirectional tests and finite element analysis results showed that the behavior of steel tubular bridge piers under bidirectional lateral loading becomes complex and exhibits a circular trajectory once local buckling occurs. The local buckling bulge in the bidirectional loading case tends to develop monotonically due to this circular trajectory. As a result, the residual deformation becomes larger. The unidirectional loading test and analysis are likely to underestimate the damage and the residual displacements caused by an earthquake. It is concluded that the effects of bidirectional lateral loading should be considered in ductility evaluation and seismic design of steel tubular bridge piers.

Keywords:steel tubular bridge piers; large displacement analysis; constant axial and cyclic bidirectional lateral loading, local buckling; strength; ductility

1. Introduction

Thin-walled steel tubular columns have found wide application as bridge piers in highway bridge systems in Japan, unlike other countries, where such structures are used much less. Steel tubular bridge piers, in contrast to concrete ones, are light and ductile. They can be built under severe constructional restrictions, such as in limited spaces in urban areas like New York and Tokyo, where effective use of limited space is greatly desired. They are also used in locations where heavy superstructures are unfavorable, such as on soft ground, reclaimed land and bay areas.

In general, because of these restrictions, steel bridge piers are designed as single columns of the cantilever type, or one to three-story frames, and they are commonly composed of rela-tively thin-walled members of closed cross-sections, either rectangular or circular in shape because of their high strength and torsional rigidity (Mamaghani 1996, Gao et al. 1998). These make them vulnerable to damage caused by coupled instability, i.e., interaction be-tween local and overall buckling, in the event of a major earthquake (Mamaghani et al. 1996a). For example, Figure 1 shows a steel bridge pier of hollow circular section, which suffered severe local buckling damage near the base of the pier in the Kobe earthquake.

When structural members are composed of thin-walled steel plate elements, the local buckling of the component plates may influence the strength and ductility of those members (Mamaghani 1997, 2006). As is well known, earthquake waves consist of three-dimensional components. Specifically, the coupling of the two horizontal components is expected to have an unfavorable effect on the ultimate behavior of steel tubular bridge piers. Therefore, it is important to examine the ultimate behavior of thin-walled steel tubular bridge piers under cyclic bidirectional lateral loading.

Cyclic circular loads are considered the severest of all bidirectional cyclic loads that can be directly compared to conventional cyclic unidirectional loads. In this study, while keeping the vertical compressive load constant, the behavior of thin-walled steel tubular bridge piers under cyclic circular bidirectional loads is examined in comparison with the behavior of such piers under cyclic unidirectional loads, shown in Figures 2 and 3. The results obtained from the cyclic bidirectional loading experiment are used to confirm the validity of geometrically and materially nonlinear finite element analysis.

2. Steel Tubular Bridge Piers

Steel tubular columns in highway bridge systems are commonly composed of relatively thin-walled members of closed cross-sections, either rectangular or circular in shape, because of their high strength and torsional rigidity (Fig. 1). Such structures are considerably different from columns in buildings. The former are characterized by: failure attributed to local buckling in the thin-walled members, irregular distribution of the story mass and stiffness, strong beams and weak columns, low rise (1-3 stories), and a need for the evaluation of the residual displacement. These make the columns vulnerable to damage caused by interaction between local and overall buckling in the event of a severe earthquake (Mamaghani 2005).

The most important parameters considered in the practical design and ductility evaluation of thin-walled steel hollow rectangular sections are the width-to-thickness ratio of the flange plate $R_f$for rectangular sections, the radius-to-thickness ratio of the circular section R_t, and the slenderness ratio of the column λ (Mamaghani and Packer 2002). While R_f and R_t influence local buckling of the section, λ controls the global stability (Mamaghani 2008, Goto 2013). They are given by:

$$R_f = \frac{b}{t}\frac{1}{n\pi}\sqrt{3(1-\nu^2)\frac{\sigma_y}{E}} \quad (\text{for box section}) \qquad \textbf{(1)}$$

$$R_t = \frac{r}{t}\sqrt{3(1-\nu^2)}\,\frac{\sigma_y}{E} \quad (\text{for circular section}) \qquad \textbf{(2)}$$

$$\lambda = \frac{2h}{r_g}\frac{1}{\pi}\sqrt{\frac{\sigma_y}{E}} \qquad \textbf{(3)}$$

in which, b = flange width; t = plate thickness; σ_y = yield stress; E = Young's modulus; ν = Poisson's ratio; n = number of subpanels divided by longitudinal stiffeners in each plate panel ($n = 1$ for unstiffened sections); r = radius of the circular section; h = column height; r_g = radius of gyration of the cross section.

The elastic strength and deformation capacity of the column due to lateral load acting at the top of column are expressed by the yield strength H_{y0}, and the yield deformation (neglecting shear deformations) δ_{y0}, respectively, corresponding to zero axial load. They are given by:

$$H_{y0} = \frac{M_y}{h} \qquad \textbf{(4)}$$

$$\delta_{y0} = \frac{H_{y0}h^3}{3EI} \qquad \textbf{(5)}$$

where M_y = yield moment and I = moment of inertia of the cross section.

Under the combined action of buckling under constant axial and monotonically increasing lateral loads, the yield strength is reduced from H_{y0} to a value denoted by H_y. The corresponding yield deformation is denoted by δ_y. The value H_y is the minimum of yield, local buckling, and instability loads evaluated by the following equations (Mamaghani 1996):

$$\frac{P}{P_u}+\frac{0.85H_y h}{M_y(1-P/P_E)}=1 \quad \textbf{(6)}$$

$$\frac{P}{P_u}+\frac{H_y h}{M_y}=1 \quad \textbf{(7)}$$

in which P = the axial load; P_y = the yield load; P_u = the ultimate load; and P_E = the Euler load.

3. Numerical Method

A series of numerical studies on the cyclic behavior of thin-walled steel tubular columns, modeling bridge piers, are carried out using the commercial computer program ANSYS (2008), and the results are compared with the experiments conducted in Japan by Obata &Goto (2004). The accuracy of the cyclic elastoplastic large-displacement finite-element analysis procedure has been verified by the experimental data. Here, as examples, analyses of the four test specimens listed in Table 1 are presented.

Cyclic circular loads are considered the severest bidirectional cyclic loads that can be directly compared to conventional cyclic unidirectional loads. Therefore, while keeping the vertical compressive load constant, the behavior of thin-walled steel tubular columns under cyclic lateral bidirectional loads is examined in comparison with this behavior under cyclic unidirectional lateral loads (Figs 2, 3).

3.1 Finite-Element Analysis

Analytical modeling of the specimen is shown in Figure 4. The shell element SHELL93 available in the commercial computer program ANSYS is used in modeling the column (Fig. 5). The SHELL93 is a three-dimensional, double-curved, eight-node shell element with six degrees of freedom per node (translations in the nodal x, y, and z directions and rotations about the nodal x, y, and z-axes). SHELL93 is particularly well suited to model curved shells. The deformation shapes are quadratic in both in-plane directions. The element has plasticity, stress stiffening, large deflection, and large strain capabilities (ANSYS, 2008).

In the analysis, the displacement convergence criterion is adopted and the convergence tolerance is taken as 10^{-5}. The details of elastoplastic large displacement analyses are reported in Mamaghani (1996). The finite-element modeling of tubular column is shown in Figure 4b. For thin-walled steel columns, local buckling always occurs near the base of the columns. Therefore, a coarse mesh discretization is employed for the upper part of the column; while finer mesh discretization is adopted for the lower part of the column to consider the effect of local buckling (Fig. 4b). The above stated mesh divisions are determined by trial and error. It is found that such mesh divisions can give an accurate result. The initial geometrical and mechanical imperfections are not considered in the analysis as their effect is insignificant on the cyclic behavior (Banno et al. 1998).

3.2 Loading History

The objective of the present study is to evaluate possible maximum deterioration in strength and ductility of thin-walled tubular steel columns caused by constant axial load and cyclic bidirectional lateral loads in comparison with conventional cyclic unidirectional loads. Therefore, cyclic bidirectional loading programs should be determined such that the results obtained by these loading programs can be directly compared to those obtained by conventional displacement-controlled cyclic unidirectional loading programs. Furthermore, in order to ensure the safety of columns, the cyclic bidirectional loading programs considered herein should be the severest ones that result in the maximum deterioration in the strength and ductility of steel columns. The practical cyclic bidirectional loading programs that have been used up to the present are the linear diagonal (BI-L), rectangular (BI-R), diamond (BI-D), and circular (BI-C) loading patterns shown in Figure 2. Circular columns exhibit isotropic behavior with respect to the *x* and *y*-axes shown in Figure 4. The displacement-controlled cyclic circular load, either with one loading cycle or three loading cycles illustrated in Figure 3, is adopted herein as one of the severest bidirectional loading programs that can be compared to conventional cyclic unidirectional loads (Fig. 2a).

While keeping the vertical compressive load constant (P/P_y= 0.15), the displacement amplitude that coincides with the radius of the loading circle is monotonically increased by the integer multiples of the initial yield displacement given by δ_{y0} (cyclic lateral displacements of increasing amplitude $\pm\delta_{y0}, \pm 2\delta_{y0}, \ldots, \pm 8\delta_{y0}$ at the top of the column). Under the same amplitude, either one loading cycle or three loading cycles are given to the columns. Most of the cyclic unidirectional loading tests conducted for thin-walled columns adopt one loading cycle, while ECCS (1986) recommends three loading cycles.

The loading specification is given in Table 3. The applied axial force P/P_y= 0.15, where P is a dead load acting at the top of the column and $P_y = \sigma_y A$ is a yield compressive strength of the column. The cyclic circular load with three loading cycles is applied to specimen PT4.5-2, while the cyclic circular load with one loading cycle is applied to specimens PT3.5-1 and PT4.5-3. For comparison, the cyclic unidirectional load with three loading cycles is applied to the specimen PT4.5-1 (Table 3).

3.3 Specimens

Specimens used in the present analysis model the hollow tubular columns of the cantilever type used for elevated highway bridge piers (Fig. 4). The specimens are made of a structural carbon steel pipe, STPG370. The measured dimensions of the analyzed columns are given in Table 1. In this table, h = column height, D = column diameter and t = tube thickness. The geometrical parameters for the specimens are also listed in Table 1. The radius-to-thickness ratio R_t has a significant influence on the ultimate behavior of circular steel columns. In the seismic design code (Japan Road Association 2002), it is specified that thin-walled circular columns should be designed such that $R_t \leqq 0.08$ in order to prevent a decrease in strength and ductility due to local buckling. The slenderness ratio parameter λ has almost the same value of approximately 0.33. The material properties of the analyzed columns are given in Table 2. In this table, σ_y = yield stress in MPa; σ_u= ultimate tensile stress in MPa; E = Young's modulus in GPa; ε_{st}^{p} = strain at the onset of strain hardening; and ν = Poisson's ratio. The uniaxial true stress-strain relation of the pipe material obtained from a tensile coupon test and the multilinear stress-strain curve used in the analysis are shown in Figure 6.

4. Numerical Results

Finite element analysis and test results for normalized lateral load (H/H_{y0}) versus lateral displacement (u/δ_{y0}) hysteretic curves in the x and y directions, the vertical displacement (u_z/u_{zy}) versus lateral displacement (u_x/δ_{y0}) hysteretic curves, and the stress distribution and buckling pattern near the base of the columns at the u_x/δ_{y0} = +5 stage of loading are plotted in Figures 7 to 11. With reference to these figures, the following observations can be made:

- The horizontal restoring force under the cyclic circular loads degrades more significantly than that under the cyclic unidirectional loads. The local buckling bulge that occurs near the base of the column causes the degradation of the restoring force. The cyclic circular loads accelerate the deformation of the local buckling bulge, compared with the cyclic unidirectional loads (Figs 7d and 10d). Under the cyclic unidirectional loads, the local buckling bulge opposite to the loading direction is stretched due to the tensile stress caused by the bending moment, and this phenomenon prevents the progress of local buckling deformation. Therefore, the performance obtained by the cyclic unidirectional loads may results in an overestimating of the strength and ductility of thin-walled steel columns.
- The envelope curve of the column subjected to three loading cycles shows a large decrease in the restoring force and ductility, compared with that subjected to one loading cycle (compare specimens PT 4.5-2 in Figure 8 and PT 3.5-1 in Figure 10 with PT 4.5-3 in Figure 9). This tendency is more significant in the post-peak range.
- By comparing specimen PT 4.5-2 in Figure 8d with PT 4.5-3 in Figure 9d in terms of the magnitude of the local buckling deformations, it can be seen that the number of loading cycles increases the deformation of the local buckling bulge. This is the main reason for the decrease in the restoring force.
- Regarding the effect of the radius-to-thickness ratio R_t, it is observed from specimens PT 4.5-3 in Figure 9d and PT 3.5-1 in Figure 10d that the column with larger R_t (PT 3.5-1) exhibits a larger local buckling bulge at the same amplitude. As a result, the strength and ductility of the column with larger R_t is reduced.

- The buckling load capacity is slightly lower in the experiment than that predicted by the analysis. This may be due to the assumed initial imperfection in the analysis. In the analysis, the cross-section out-of-straightness and residual stress is not accounted for. It is worth noting that the previous research by the author indicates that under cyclic loading the initial residual stresses and initial section imperfection decrease the initial stiffness and initial buckling load capacity, in a similar way to that in a monotonic loading, and have almost no effect on the subsequent cyclic behavior of the member (Mamaghani et al. 1996b, Banno et al. 1998).
- An example of the deformation of the specimen for test and analysis at the u_x/δ_y = +5 stage of loading is shown in Figures 7c and 7d, respectively. Both the test results and analytical results indicate that pronounced yielding and local buckling occur near the base of the column. The buckling pattern of the column is well simulated.
- The numerical results reveal that the degradation in the compression strength of the column increases with the number of cycles and the amplitude of deformation. The effects of local-buckling progress can also be observed from the results in Figures 7 to 10 as the strength decreases with the increase in displacement amplitude.
- A comparison between hysteresis loops in Figures 7 to 10 shows that there is a reasonably good agreement between analytical results and experiments. An observed small discrepancy between experimental and analytical hysteresis loops is that the predicted cyclic load capacities are slightly higher than those of the experiment. The possible reasons are: (a) the multilinear kinematic hardening material model adopted in the analysis does not accurately consider the reduction of the elastic range due to plastic deformation (Bauschinger effect). In this model the size of elastic range is taken to be constant, which does not represent the actual behavior of structural steel (Mamaghani et al. 1995, Shen et al. 1995). More accurate results can be obtained from analysis using a cyclic constitutive law representing the more realistic behavior of the material; and (b) in the analysis the cross-section's out-of-straightness and residual stresses, which affect the initial buckling load, are not considered.
- The vertical displacement caused by the local buckling bulge is accurately predicted by the finite element analysis, see Figure 7b, 8c, 9c, and 10c.
- In contrast to the numerical results under the cyclic circular load with one loading cycle, there is some small discrepancy between the experimental and numerical results for three loading cycles. This is primarily due to the fact that a larger inelastic deformation occurs in the specimens subjected to three loading cycles, compared with those subjected to one loading cycle. That is, the maximum equivalent plastic strains accumulated in the specimens under three loading cycles are larger than those of the one loading cycle.

5. Conclusions

This paper deals with the seismic performanceandstability evaluation of thin-walled steel tubular bridge piers subjected to cyclic lateral bidirectional loading in the presence of constant axial load. The multilinear kinematic hardening model is employed for material nonlinearity in the elastoplastic finite-element analysis of piers. The bidirectional tests are used to substantiate the accuracy of the finite-element analysis. A reasonably good agreement between the experiment and the analysis confirms the validity of the finite-element modeling adopted in this study. The results confirm the importance of considering bidirectional lateral loading in steel tubular bridge piers. From the bidirectional pseudodynamic tests and analysis results, it is concluded that the behavior of a specimen under lateral bidirectional loading becomes complex and exhibits a circular trajectory once local buckling occurs. The local buckling bulge in the lateral bidirectional loading case tends to develop continuously due to the circular trajectory causing larger residual deformation. The cyclic unidirectional lateral loading test underestimates the damage and the residual displacements caused by an earthquake. The results revealed that the importance of bidirectional lateral loading should be considered in the seismic design of steel tubular bridge piers.

References

ANSYS (2008). "User's manual", Version 11, ANSYS Structural Analysis Guide, ANSYS Inc.

Banno, S., I. H.P. Mamaghani, T. Usami, E. Mizuno (1998)."Cyclic elastoplastic large deflection analysis of thin steel plates", Journal of Engineering Mechanics, ASCE, 124(4), 363-370.

ECCS (1986)."Recommended testing procedure for assessing the behavior of structural steel elements under cyclic load", Japan Road Association (2002). Specification for road bridges and commentaries: V. Seismic design. Tokyo (in Japanese).

Gao, S., Usami, T., Ge, H. (1998) Ductility Evaluation of Steel Bridge Piers with Pipe Sections, Journal of Engineering Mechanics, ASCE, Vol. 124, No. 5, pp. 260-267.

Goto, Y. (2013) Seismic Design of Thin-walled Steel and CFT Piers, Bridge Engineering Handbook, Second Edition: Seismic Design, Edited by Wai-Fah Chen, LianDuan, pp. 337-380.

Mamaghani, I.H.P. (2008). "Seismic Design and Ductility Evaluation of Thin-Walled Steel Bridge Piers of Rectangular Sections", Journal of the Transportation Research Board, No. 2050, Washington D.C., pp. 137-142.

Mamaghani, I. H. P. (1996)."Cyclic elastoplastic behavior of steel structures: theory and experiment", Ph.D. Thesis, Nagoya University, Nagoya, Japan.

Mamaghani, I. H. P., C. Shen, E. Mizuno, and T. Usami (1995)."Cyclic behavior of structural steels.I: experiments", J. Engrg. Mech., ASCE, 121(11), 1158-1164.

Mamaghani, I. H. P., T. Usami, and E. Mizuno (1996a). "Inelastic large deflection analysis of steel structural members under cyclic loading", Engineering Structures, UK, Elsevier Science, 18(9), 659-668.

Mamaghani, I. H. P., T. Usami, and E. Mizuno (1996b). "Cyclic elastoplastic large displacement behaviour of steel compression members", J. Structural Engineering, JSCE, Vol. 42A, 135-145.

Mamaghani, I. H. P., T. Usami, and E. Mizuno (1997)."Hysteretic behavior of compact steel rectangular beam-columns", Journal of Structural Engineering, JSCE, Japan, Vol. 43A, 187-194.

Mamaghani, I.H.P. (2006). "Inelastic Cyclic Analysis and Stability Evaluation of Steel Braces", Structural Stability Research Council, February 8-11, San Antonion, Texas, pp. 281-300.

Mamaghani, I.H.P. 2005."Seismic performance evaluation of thin-walled steel tubular columns", Structural Stability Research Council, Montreal, Quebec, Canada.pp.489-506.

Mamaghani, I.H.P., Shen, C., Mizuno, E., Usami, T. (1995)."Cyclic behavior of structural steels. I: experiments", Journal of Engineering Mechanics, ASCE, USA, Vol.121, No.11,1158-1164.

Mamaghani, I.H.P, and Packer, J.A. (2002). "Inelastic Behavior of Partially Concrete-Filled Steel Hollow Sections", 4th Structural Specialty Conference of the Canadian Society for Civil Engineering, Montréal, Québec, Canada, s71.

Obata, M., and Goto, Y. (2004)."Development of 3D pseudo-dynamic experiment system for bridge piers and columns", J. Struct. Mech. Earthquake Eng., JSCE, No. 753/I-66, 253–266 (in Japanese).

Shen, C., Mamaghani, I.H.P., Mizuno, E. and Usami, T. (1995)."Cyclic behavior of structural steels.II: theory", Journal of Engineering Mechanics, ASCE, USA, Vol.121, No.11, 1165-1172.

Table1. Geometry of analyzed specimens

Specimen	h (mm)	D (mm)	t (mm)	R_r	λ
PT4.5-1	1460	251	4.7	0.068	0.34
PT4.5-2	1460	259.2	4.6	0.071	0.33
PT4.5-3	1460	259.2	4.5	0.073	0.33
PT3.5-1	1460	258.2	3.5	0.093	0.32

Table2. Material properties

Specimen	E (GPa)	v	σ_y (MPa)	σ_u (MPa)	ε_{st}^{p}
PT4.5-1	206	0.3	325	592	0.01
PT4.5-2	206	0.3	325	592	0.01
PT4.5-3	206	0.3	321	579	0.01
PT3.5-1	206	0.3	321	579	0.01

Table3. Loading specifications

Specimen	H_{ro} (kN)	δ_{ro} (mm)	P/P_r	Loading Program
PT4.5-1	44	5.34	0.15	Unidirectional 3
PT4.5-2	46.6	5.24	0.15	Circular 3
PT4.5-3	43.9	5.07	0.15	Circular 1
PT3.5-1	34.5	4.92	0.15	Circular 1

Fig. 1. Local buckling of steel bridge pier, Kobe Earthquake, January 1995.

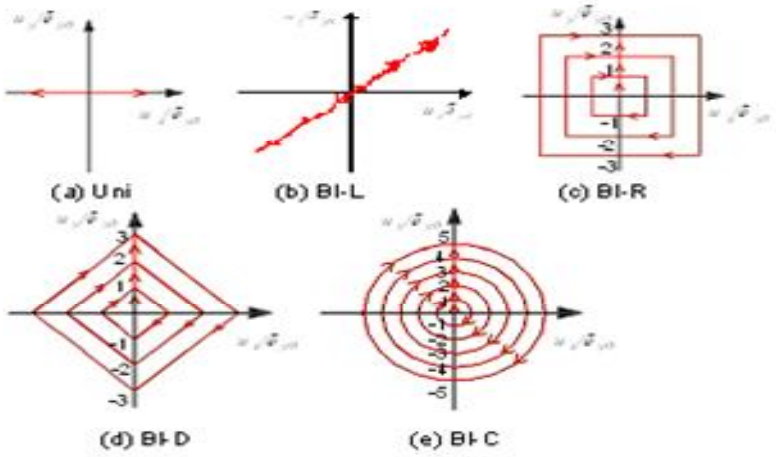

Fig. 2- Cyclic loading patterns: (a) Unidirectional (Uni), (b) Bidirectional-linear (BI-L), (c) Bidirectional rectangular (BI-R), (d) Bidirectional-diamond (BI-D), and (e) Bidirectional-circular (BI-C)

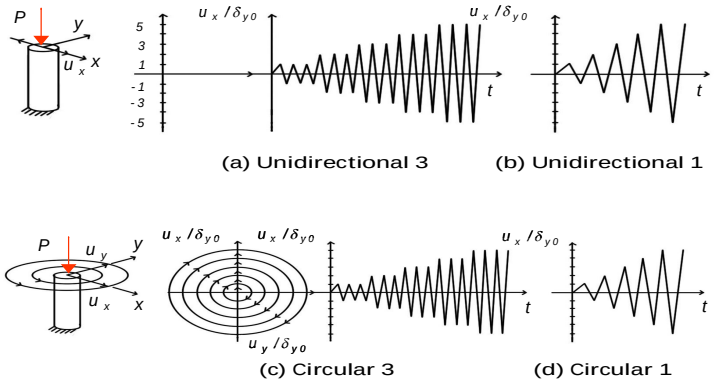

Figure 3: Loading programs

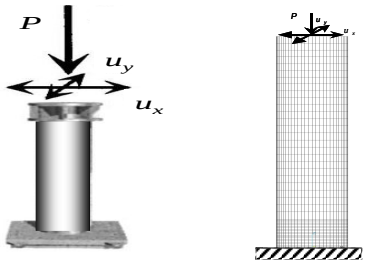

Figure 4: (a) Steel Tubular Column, (b) Finite Element Modeling

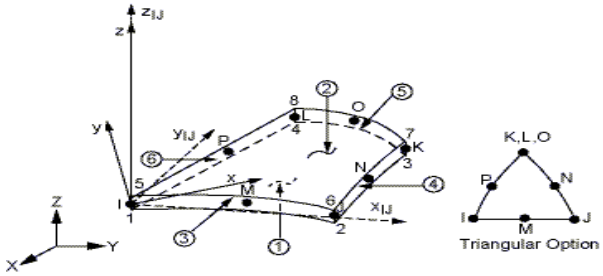

Figure 5: Element SHELL93

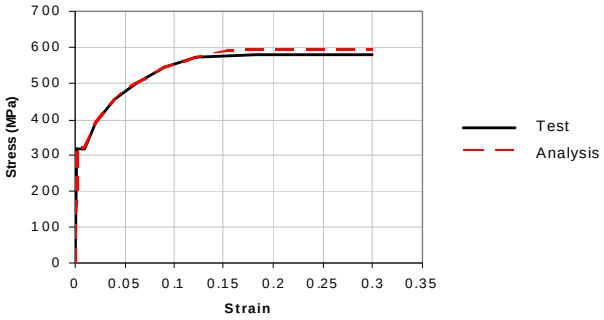

Figure 6: Uniaxial Stress-Strain Relation of the Material and the Multilinear Stress-Strain Curve Used in the Analysis (STPG370)

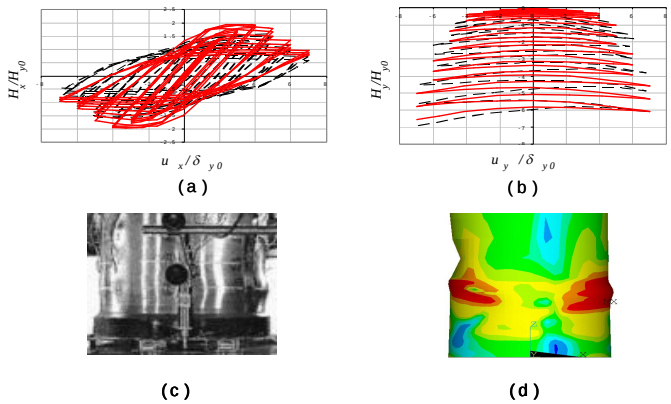

Figure 7. Comparison of hysteretic loops between experiment and analysis for column PT4.5-1, (a) normalized lateral load versus lateral displacement in x direction, (b) normalized lateral load versus lateral displacement in y directions, (c) buckling pattern near the base of the column from the test at $u_x / \delta_{y0} = +5$, (d) stress distribution and buckling pattern near the base of the column from the analysis at $u_x / \delta_{y0} = +5$.

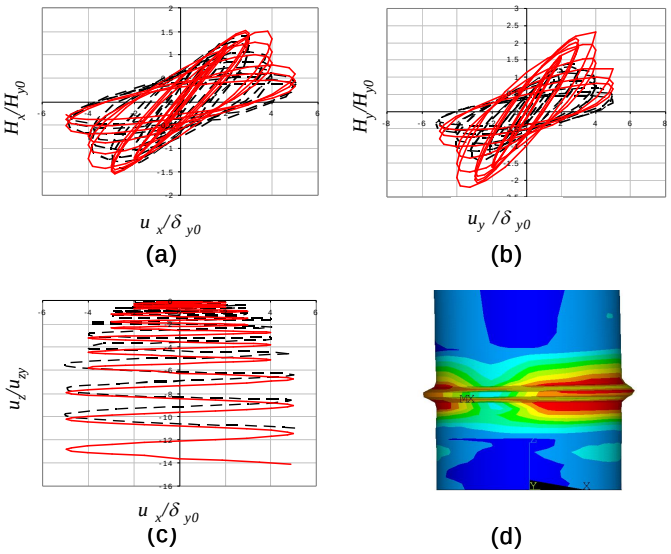

Figure 8. Comparison of hysteretic loops between experiment and analysis for column PT4.5-2, (a) normalized lateral load versus lateral displacement in x direction, (b) normalized lateral load versus lateral displacement in y directions, (c) normalized vertical load versus vertical displacement in z direction, (d) stress distribution and buckling pattern near the base of the column at $u_x/\delta_{y0} = +5$.

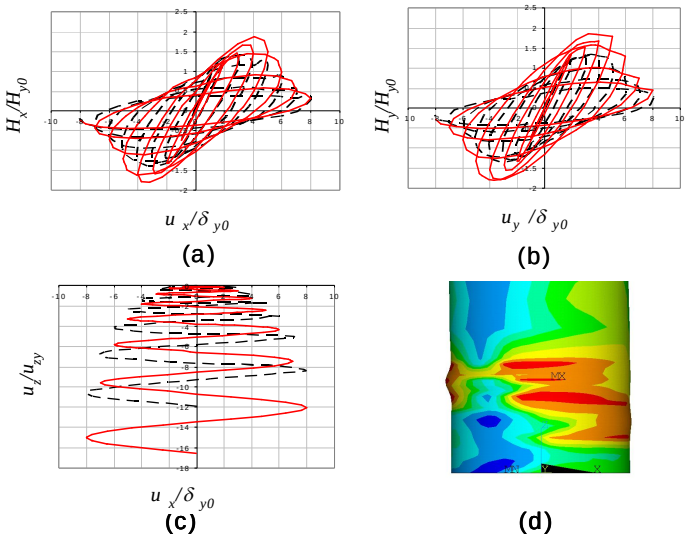

Figure 9. Comparison of hysteretic loops between experiment and analysis for column PT4.5-3, (a) normalized lateral load versus lateral displacement in x direction, (b) normalized lateral load versus lateral displacement in y directions, (c) normalized vertical load versus vertical displacement in z direction, (d) stress distribution and buckling pattern near the base of the column at $u_x/\delta_{y0} = +5$.

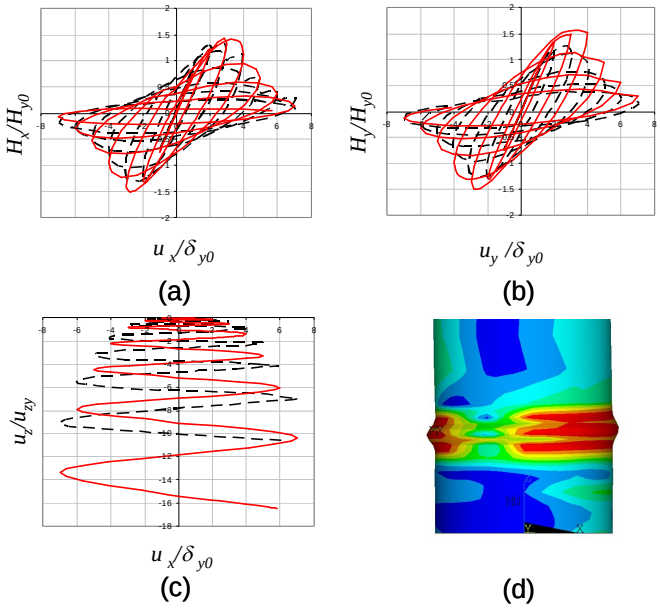

Figure 10. Comparison of hysteretic loops between experiment and analysis for column PT3.5-1, (a) normalized lateral load versus lateral displacement in *x* direction, (b) normalized lateral load versus lateral displacement in *y* directions, (c) normalized vertical load versus vertical displacement in *z* direction, (d) stress distribution and buckling pattern near the base of the column at $u_x / \delta_{y0} = +5$.